



Process capability factors in micro-hole drilling of BGA board materials

By Tony Bannan, Chris Gerrard, Mike Wellstead

This paper was presented at the EIPC Winter Conference, Budapest, 26-27 January 2006

High levels of machine and process capability are demanded to ensure manufacturing productivity in BGA and CSP-type circuit systems. The factors determining capability include drilling machine axis control, configuration of the cutting tool and gripping arrangement, integrity of work holding and precision of drilling spindle. The contribution of these elements is analyzed and reported.

1 Introduction

The drilling spindle used in the PCB drilling machine is a high-precision motorised-bearing unit with one primary, essential function: to rotate the drill-bit as accurately as possible, with respect to both speed and geometric uniformity, in order to drill the required hole as productively and as precisely as possible. Due to the speed ranges required, most modern PCB drilling systems utilise air bearings, allowing for very low friction, high stiffness and low geometric runout. Speed and torque control are essential to enable a range of drill sizes to be used effectively. A brief description of the air-bearing spindle is provided in section 2.



PCB drillers and OEMs utilise a wide range of techniques to quantify hole registration accuracy and a common statistical control method used is the calculation of the *process capability*, commonly referred to as C_{pk} . Since it is relevant to the context of this paper, a short recap of process control principles is given in section 3.

Process capability is a critical validation measure and is often used by OEMs and PCB drillers alike to qualify a particular drilling process or machine system. The classic 'dartboard' graph is a common feature in acceptance trials, this graph indicating the degree of scatter around a nominal target point. As such, it is essential that the machine and process elements contributing to the process capability parameter are understood. Section 4 separates and defines some of these elements and explains their role in the total 'system', and conclusions are drawn in section 5.

2 The basics of aerostatic bearing geometry

Figure 1 (below) illustrates a typical air bearing journal used in PCB drilling spindles.



Figure 1 Typical journal bearings

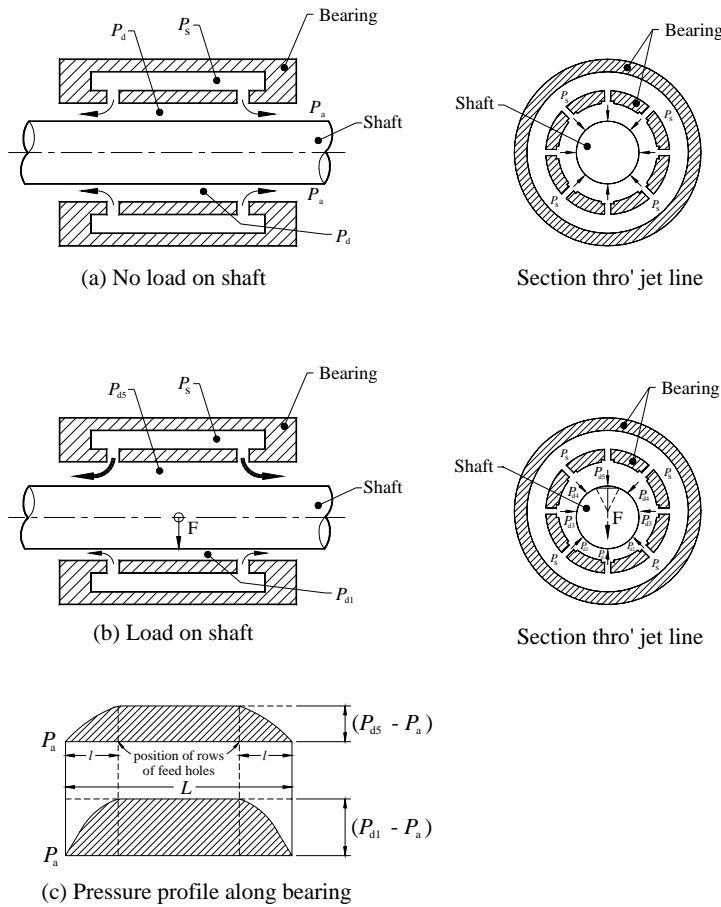


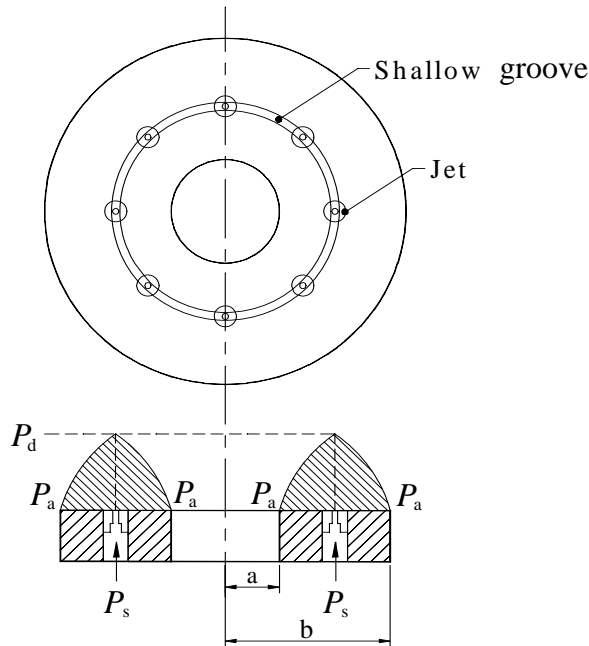
Figure 2 Radial geometry in aerostatic bearings



With reference to Figure 2a, compressed air at approximately 5.5 bar pressure is supplied through tiny jets around the internal bore of the radial bearing into the narrow gap between the shaft and the bearing, thus allowing the shaft to float freely on the bearing centreline. When a side load is exerted on the shaft, as in Figure 2b, the shaft is forced off-centre causing a larger gap to exist on one side of the bearing and a reduced gap on the other. The smaller gap reduces the air flow on that side, automatically raising the localised air pressure, and hence prevents further movement of the shaft due to the load. The bearing system is now in equilibrium again as shown in Figure 2c, the difference between the two pressure profiles being equal to the applied load.



Figure 3 View of axial bearing plate



Pressure profile across axial bearing

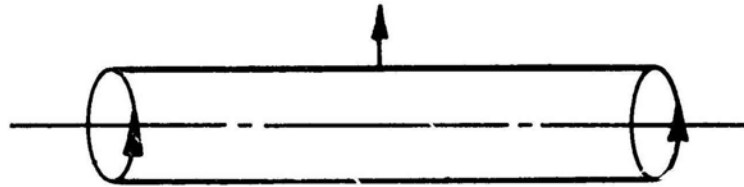
Figure 4 Axial/thrust geometry in aerostatic bearing



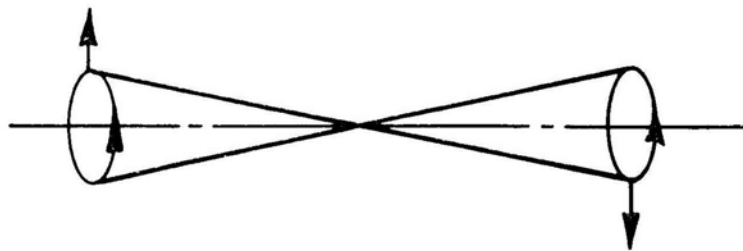
In a similar way to the radial bearing, compressed air flows through tiny jets equally spaced around a diameter in the axial bearing plate as shown in Figure 3, and subsequently into a small gap between the shaft runner face and the bearing plate. As there are two axial bearing plates attached in opposition, with the shaft runner sandwiched in-between, the shaft is able to float freely on the air film. If an axial load is applied to the shaft, the gap reduces on one side of the runner, reducing the air flow and hence increasing the pressure, which resists the applied load. The air flows both radially outwards and inwards across the axial bearing plate, as shown on the pressure profile in Figure 4.

In a typical PCB drilling spindle, the shaft will be supported by two radial bearings fitted either side of a centrally mounted electrical motor, with an axial bearing system located at one end of the shaft.

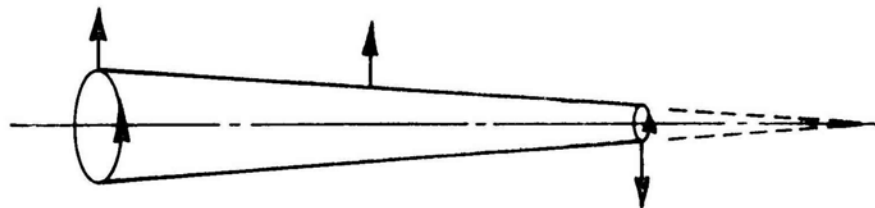
As with any rotating shaft system, air bearing drilling spindles encounter resonant frequencies and vibrational effects across the speed range. The effect on shaft motion must be minimized by careful design and precision balancing. The impact on shaft orbit is shown in Figure 5 (below), and this error motion will be transferred onto the drill bit clamped in the collet in the front of the shaft. The amplitude of the motion will vary according to the shaft speed, and the stiffness/damping characteristics of the bearing system. As the drill bit extends significantly forward of the end of the shaft, it is obvious that even small displacements, due to the combination of the conic and cylindrical motions within the bearing system, may result in much greater motions at the tip of the drill depending on the vector angles involved.



(a) Cylindrical whirl generated by static unbalance force



(b) Conical whirl generated by dynamic unbalance couple



(c) General form of whirl generated by residual static and dynamic unbalance

Figure 5 Effects of residual unbalance on shaft motion

Figure 6 illustrates the impact of residual unbalance and bearing resonant frequencies on the radial vibration of a spindle and the dynamic runout of a checking pin held in the collet. In this example the DRO starts at approx. $2.5\mu\text{m}$ at very low speed and gradually reduces to a minimum of about $1\mu\text{m}$ at full speed (250,000 rpm). However, it will be noticed that at about 150,000 rpm, there is a spike in both vibration and DRO traces, which is due to reduced bearing damping at the bearing resonant frequency. This is a phenomenon that is inherent in all high speed air bearing spindles to some degree, and is affected by many different design parameters. Once through this critical speed, the shaft is less sensitive to residual imbalance and hence both vibration and DRO tend to reduce dramatically with further increase in speed, up until the approach of 'half speed whirl'. This resonant condition, indicated by a very rapid rise in both values, cannot be surpassed and tends to dictate the maximum rotational speed of the spindle design.



It is this mechanism that dictates the dynamic performance of the spindle, and hence the drill bit, and is a critical part of the accuracy of the drilling process.

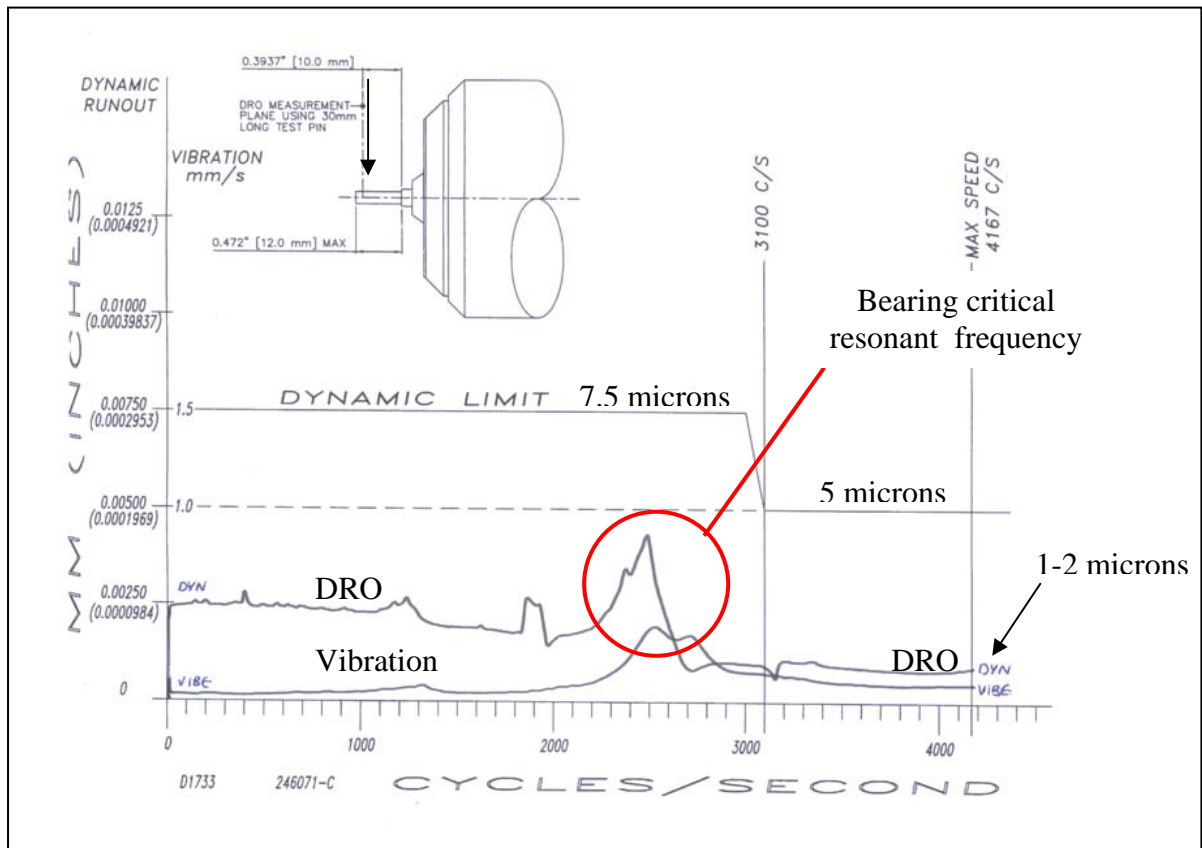


Figure 6 Typical spindle vibration and dynamic runout traces

3 Process controls and capability evaluation

A clear understanding of the mechanisms and principles described above underpin successful spindle design, and high geometric precision and good production controls are essential in the manufacturing of spindles. The influence of inherent dynamic runout and orbit control on the actual performance of the spindle is significant. However, there are other factors, and a brief summary of the foundation of process capability, C_{pk} , is helpful.

C_{pk} is closely related to the capability index C_p . It is important to recognise that capability indices estimates are valid only if the sample size used is 'large enough'. Large enough is generally thought to be at least 50 independent data values, but may need to be much higher depending upon the data requirements. The general equation for the capability index, for a normally distributed population, C_p , is:



$$C_p = \frac{USL - LSL}{6s} \quad (1)$$

In equation (1) USL and LSL are upper and lower specified limits respectively, and s is standard deviation. This equation defines the measure of our process capability as a proportion of the observed process variation covered by the process specifications. In this case the process variation is measured by 6 standard deviations (+/- 3 on each side of the mean). Clearly, if $C_p > 1.0$, then the process specification covers almost all of our process observations.

One of the main problems with the C_p index is that it is concerned with *spread* or *range* of observations, and does not indicate a process that has drifted away from 'centre'. To account for this the equation is modified in such a way as to indicate both the spread of observations and their degree of centering around the process 'target'. This index, known as C_{pk} , is therefore a more useful term in qualifying the overall capability of the process.

$$C_{pk} = \min \left[\frac{USL - x_m}{3s}, \frac{x_m - LSL}{3s} \right] \quad (2)$$

In equation (2) x_m is the numerical process mean. C_{pk} is therefore the minimum distance between the specification limits and the process mean divided by 3 standard deviations. It is possible to find that for a highly repeatable, low-spread process the C_{pk} value is less than the C_p value; this occurs when the process distribution is not centered between the specification limits.

4 Machine elements and component sub-systems

The contribution to total process capability made by the spindle will be significant. If the board requirement specification for a particular manufacturer demands $100\mu\text{m}$ holes at pitch-spacing of $150\mu\text{m}$, the distance between the hole edges is nominally $50\mu\text{m}$. Neglecting dynamically-induced bending and whirling effects of the drill-bit – and the multiplying effect of the length of the drill-bit - a fully transmitted DRO of $5\mu\text{m}$ in the spindle has the potential to increase the hole diameter by $5\mu\text{m}$, thereby reducing the hole edge distance to $40\mu\text{m}$. This dynamic error, taken together with other sources of error within the machine and the work-holding system, can lead to further, significant deterioration in the capability of the process.

For this reason, spindle manufacturers and PCB drilling machine OEMs go to great lengths to quantify and minimise such sources of error and, as is the norm with machine tools, a design capability well in excess of the demands of the application is common.

PCB drilling systems are therefore equipped with extremely high precision sub-systems and components, and built to the highest standards. This section briefly describes the critical sub-systems involved and highlights some of the considerations in design, including machine axis control, drill-bit configuration and drill-bit gripping method. Assistance with the graphical representations has been generously provided by Union Tool Company, Nagaoka, Japan.

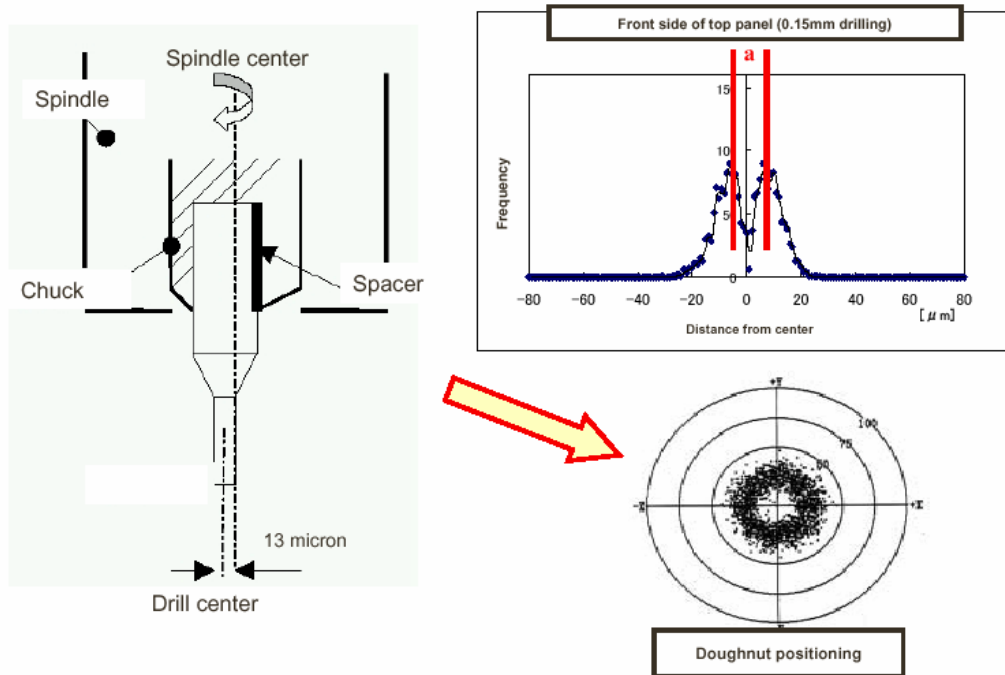


Figure 7 Positioning errors due to inaccurate tool-holding

In the example, provided in Figure 7, a radial error of $13\mu\text{m}$ is induced by the insertion of a spacing shim, simulating a tool load error. This error could be caused by localised damage to the drill shank or collet internal diameter, or simply by the pick-up of debris such as dirt or process swarf from the board material. Although the example exaggerates the error, it can be seen that a relatively small geometric displacement has a significant impact on the drill positioning. In this case, the whole drill-bit is effectively 'thrown' off centre, causing the drill entry point (into the top layer of the board) to be mis-targeted. Due to the inherent compliance (ability to bend) of the extremely fine drill-bit, it will tend to follow its entry point, resulting in a hole distribution similar to the 'doughnut' shown on the graph. The magnitude of this error will be difficult to define, however in this case it is clear to see that an absolute deviation of at least $20\mu\text{m}$ would result, inevitably having a devastating effect on the C_{pk} index achieved.

In addition to the ingress of foreign materials to the tool-holding system, there is an inherent tendency for the chuck to reduce its grip on the drill shank, allowing further dynamic runout, as the spindle system accelerates to a high speed. This is a result of the high, dynamically-induced centripetal forces, which deflect the retaining walls of the spindle shaft and cause the collet retaining mechanism (normally based on a spring

system) to become elastically strained. In order to accommodate this factor, current designs subject the tool mechanism to very high static pre-load forces, giving extremely high static grip torque.

In the next example, in Figures 8 and 9, the impact of machine motion errors is illustrated. Motion errors can emanate from a wide variety of sources, including:

- Servo positioning / axis interpolation
- Programming or machine offsets
- Axis misalignment
- Vibrations (environmental and machine induced)
- Necessary clearance / backlash in the machine motion elements (ballscrews, nuts, bearings, slideways etc.)
- Physical wear in the machine motion elements

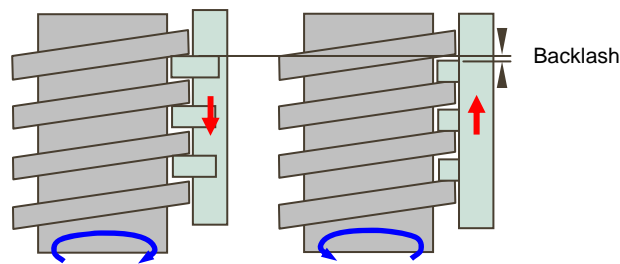


Figure 8 Positioning errors due to machine axis motions

Figure 9 is a simplified illustration of motion error due to backlash, which is present in all conventional lead/ballscrew driven systems. Backlash elimination systems are of course actively helpful in minimising such errors – at least in the newly adjusted machine - but a small amount of clearance caused by wear or loss of pre-load emerges with use. Alternative machine designs with linear motor technologies have a lower incidence of physical degradation, however they still utilise mechanical/rolling element slide systems which are subject to wear.

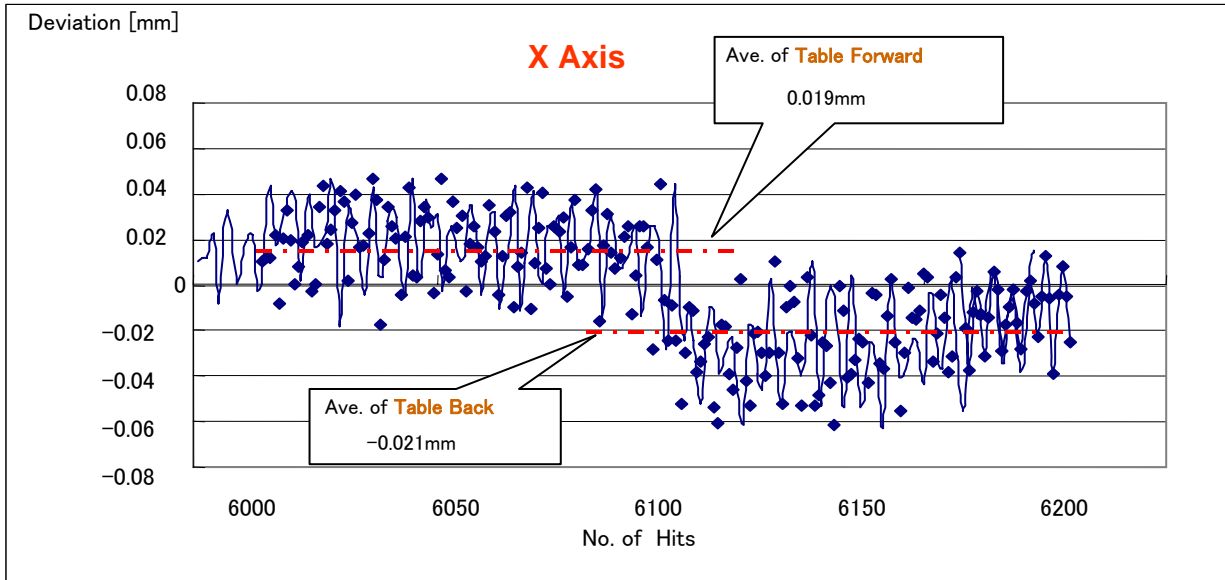
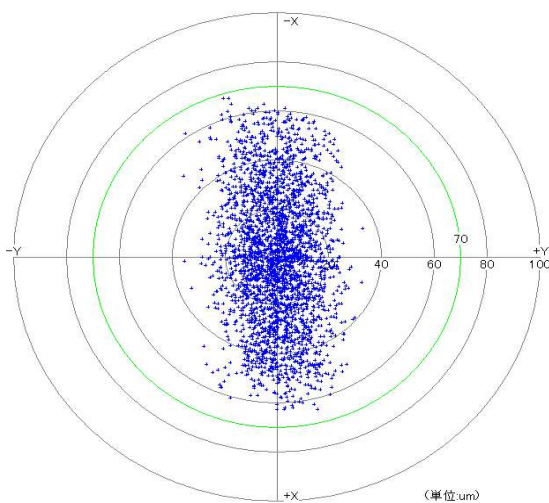


Figure 9 Magnitude of deviations due to X-axis positioning

The value of backlash illustrated in Figure 8 is equivalent to the distance between opposite screw flanks when the direction of screw rotation is reversed. In this case, a notional clearance (at a local point on the X-axis) of $40\mu\text{m}$ will generate an attendant displacement in the drill positioning. In practice, a value nearer to $8\mu\text{m}$ is common. Even with this ‘small’ amount, the result will be a ‘stepped’ reversal graph, as shown in Figure 10 (above), with the X position of the hole directly affected by the feed direction of the drill-head / work-table.



On the ‘dartboard’ graph (Figure 10, left) the resulting hole distribution will appear elongated in the direction of the error motion – in this case along the X-axis. This shape of distribution can clearly be seen on the graph. The high observation range defines a proportionally high value of deviation, with a correspondingly damaging impact on the C_{pk} index. Again, it can be seen that even a quite subtle error can have a disproportionately negative effect on the end product.

Figure 10 ‘Skewed’ X-axis hole scatter



Further debate exists around the use of shank-rings on PCB drills. They are widely implemented and have a range of strengths and weaknesses, however their contribution to the error budget needs to be considered. The main benefits provided by a shank-ring are physical depth control (e.g. referencing after re-grind) and the shielding effect helping to reduce the ingress of debris into the spindle chuck.

The main disadvantage of the shank-ring is its overhung mass effect, contributing to increased dynamic runout at the tip of the drill-bit. Drills with and without shank rings are illustrated in Figure 11 (right). Conversely, the drill without the shank-ring provides a lower overhung mass and eliminates the additional dynamic runout associated with this. It does however have the disadvantage that spindle shielding and sealing is not assisted by the presence of a ring. Depth and drill-point re-positioning has to be done entirely by the drilling machine's length measurement system or auto-offset control. This is however common practice amongst advanced machines and does not present a material disadvantage. The relative performance (with respect to hole registration accuracy) of these configurations is shown in Figure 12 (below).

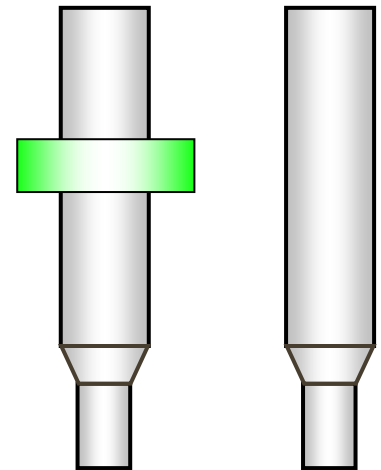


Figure 11 Drill shank-rings

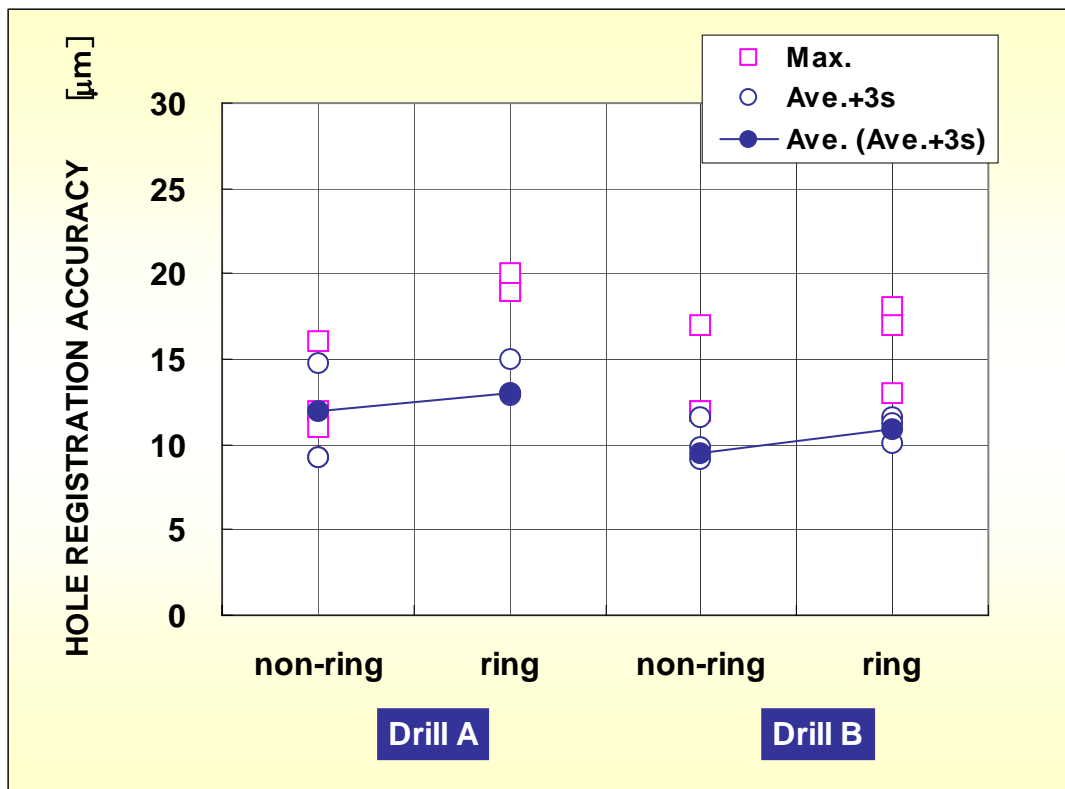




Figure 12 The influence of drill shank-rings on hole registration

A study undertaken by Union Tool Company attempted to quantify the effect of drill shank-rings, both on the incidence of drill breakage and on registration accuracy. In the case in point, the issue of interest is of course positional accuracy, and their findings are of interest. The conditions established for the trials were as follows:

- Drill diameter 0.105mm
- Panel 0.1mm thick
- Stack height x4
- Spindle speed 200 x 10³ rpm
- Sample size 3 off Type A drills (no ring)
 3 off Type A drills (with ring)
 3 off Type B drills (no ring)
 3 off Type B drills (with ring)
- Hit count 3000 hits each

For the purposes of the analysis, the basis for this trial is an individually selected, virtually zero runout spindle, providing an objective assessment that the major error contribution is made by the tool rather than the spindle or gripping system. Inevitably, there is significant interaction between the systems, however for purposes of the trial the spindle factors are neglected.

It is evident from Figure 12 that the registration accuracy within the sample is negatively affected by the addition of a drill shank-ring. Drill A's maximum error without the shank-ring varies between < 12 μ m to <16 μ m. With the addition of the shank-ring the maximum error range is >18 μ m to approximately 20 μ m. Drill B's registration accuracy values show a similar pattern. The result is that the whole sample averaged values indicate 3 μ m deterioration in registration accuracy when a drill shank-ring is installed. Even without the shank-ring, there will be a quantity of runout inherent in the drill action at the operational speed. Again, although this is a relatively small amount, when added to the other potential sources of error in the total system, it can play a significant role in the erosion of the overall process capability.

5 Conclusions

The information presented and discussed here is intended to illustrate the actual and potential sources of error present in a PCB production drilling system. In the measurement and definition of C_{pk} in a machine acceptance and production environment, these sources and factors should be considered.



Hole registration accuracy in modern PCB systems is becoming increasingly more demanding, particularly in smaller micro-via and densely populated technologies such as BGA and CSP boards, where a requirement of $C_{pk} > 5$ is increasingly common. In 'standard' PCBs, it is not uncommon to have a positioning accuracy requirement of $30\mu\text{m}$ maximum deviation, with repeatability well inside this. For such high levels of C_{pk} requirement, only a small portion of this tolerance band is available, and 'stray' holes approaching the USL and LSL will disproportionately skew the capability figures in a negative direction.

In the examples given throughout this presentation, using the more practical case scenarios rather than the worst case possibilities, a total potential error of $36\mu\text{m}$ – of which $5\mu\text{m}$ is due to the spindle at critical frequency - could be transferred to the top layer of the board. When through this region, with the spindle running at its design speed, the runout contribution will be in the order of $<2\mu\text{m}$. Allowing for uncertainty, and for care taken in every aspect of set-up, even if only one third of this tolerance is used in a reasonably centred process, the C_{pk} will be in the region 1.8 to 2.2, which is still well below many drillers' expectations.

In conclusion, great care should be taken when assigning C_{pk} values to controlled processes where a combination of contributing factors can be found.

For more information on this article or on Westwind products, please contact:

Tony Bannan, Technical Director (email: tbannan@gsig.com)

Chris Gerrard, R&D Manager (email: cgerrard@gsig.com)

Mike Wellstead, Applications Manager (email: mwellstead@gsig.com)

Westwind Air Bearings, a division of GSI Group Ltd.

Holton Road, Holton Heath

Poole, Dorset. BH16 6LN. UK

Tel: +44 (0)1202 627200

Fax: +44 (0)1202 627202

www.westwind-airbearings.com